Nonhydrostatic Atmospheric Modeling Using a Combined Cartesian Grid

Hiroe Yamazaki and Takehiko Satomura
Kyoto University, Kyoto, Japan

Oct 26, 2009 @ SRNWP-WS

Ladies and gentlemen. Today, I will be talking about nohydrostatic atmospheric modeling using a combined Cartesian grid.

This study explores the development of a new numerical model for ultra-high resolution simulations using Δx = O(10) m.

- Steep slopes are represented over mountainous and urban areas.
- Commonly-used terrain-following approach induces large errors around steep slopes.

Another representation method of topography is required for ultra-high resolution models.

In this study, we are developing a new numerical model for ultra-high resolution simulations at horizontal grid intervals of less than 100 meters. First let me mention briefly why we decided to conduct the present study. We consider that the representation of topography in models as one of the important issues for high resolution simulations, because an increase in horizontal resolution introduces steep slopes over mountainous and urban areas. However, the commonly used terrain following representation of topography induces large truncation errors around steep slopes. Thus we think that another representation method of topography is required for ultra-high resolution models, and we explore the development of an atmospheric model for simulating flows over complex terrain including steep slopes.

Terrain-following approach
(e.g., MM5, WRF, NICAM)

Equations are discretized on a grid that conforms to the lower boundary.

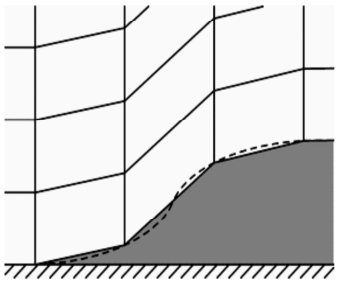

- The imposition of the lower boundary condition is greatly simplified.
- Truncation errors due to nonorthogonality lead to artificial circulations around steep slopes.

So first, we take a look at the commonly-used terrain-following approach. This approach is used in many models including MM5, WRF, NICAM and so on. Here, equations are discretized on a grid that conforms to the lower boundary. The main advantage of this approach is that the imposition of the lower boundary condition is greatly simplified. However, horizontal gradient computation on a terrain-following grid is essentially subject to truncation errors due to nonorthogonal coordinates. In particular, inaccurate evaluation of the pressure gradient leads to artificial circulations around steep slopes.

2-D mountain wave simulations using a terrain-following model (Satomura, 1989)

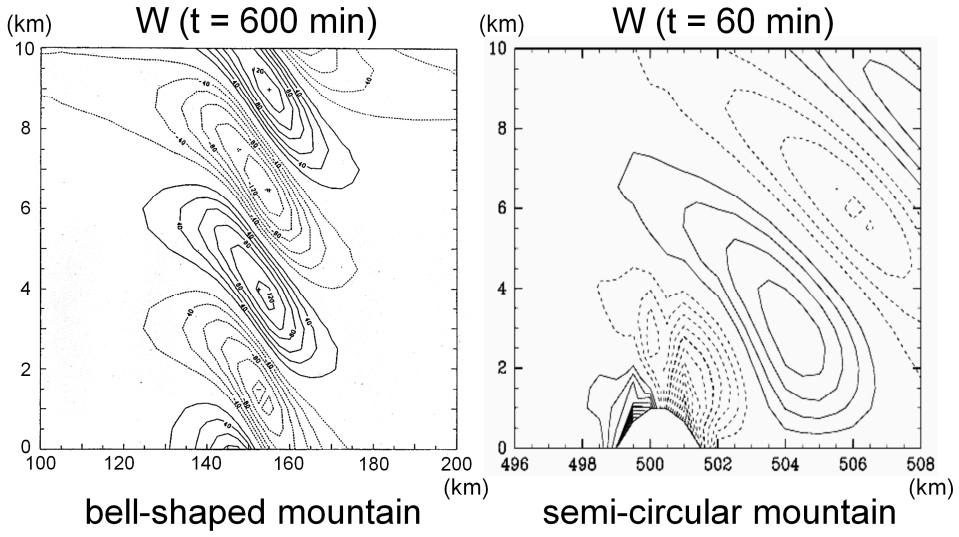

For example, two-dimensional numerical simulations of flow over a mountain using a terrain following model were performed by Satomura. Two mountains were used, one was a gently sloping bell-shaped mountain and the other was a semi-circular mountain which had steep slopes at the foot. The results of vertical velocity fields are shown here. In the case of the bell-shaped mountain, the terrain following model reproduced smooth and accurate mountain waves. On the other hand, in the case of the semi-circular mountain, the reproduced vertical velocity field was discontinuous because of the truncation errors due to the slantwise intersection of grid lines around steep slopes. We cannot ignore these near-ground errors because they have a critical impact on predictions of clouds and rain.

We developed a new 2-D nonhydrostatic atmospheric model using Cartesian coordinates code-named “Sayaca-2D”.

- Fully compressible quasi-flux form equations are used as governing equations.
- The shaved cell method based on finite-volume discretization is used.
- A cell-combining approach is used that employs a unique variable arrangement.

So in the present study, we developed a new two-dimensional nonhydrostatic atmospheric model using Cartesian coordinates instead of using terrain-following coordinates. The name of our model is “Sayaca-2D”. “Sayaca” is a Japanese girl’s name. We used fully compressible quasi-flux form equations as governing equations. As a method for representing topography on a Cartesian grid, we used the shaved cell method based on finite-volume discretization. A unique feature of our model is that we used a cell-combining approach that employs a unique variable arrangement, which I will discuss in detail later.

Governing equations
(Satomura & Akiba, 2003)

$$\frac{\partial(\rho u)}{\partial t}+\frac{\partial(\rho uu)}{\partial x}+\frac{\partial(\rho uw)}{\partial z}=-\frac{\partial p'}{\partial x}+DIF(\rho u)$$
$$\frac{\partial(\rho w)}{\partial t}+\frac{\partial(\rho wu)}{\partial x}+\frac{\partial(\rho ww)}{\partial z}=-\frac{\partial p'}{\partial z}-\rho' g+DIF(\rho w)$$
$$\frac{\partial p'}{\partial t}=-\frac{R_d\pi}{1-R_d/C_p}\left\{\frac{\partial(\rho\theta u)}{\partial x}+\frac{\partial(\rho\theta w)}{\partial z}+DIF(\rho\theta)\right\}$$
$$\frac{\partial \rho'}{\partial t}+\frac{\partial(\rho u)}{\partial x}+\frac{\partial(\rho w)}{\partial z}=0$$

- Quasi-flux form fully compressible equations
- Well suited to finite-volume discretization in the view of conservation characteristics.

Now, I will explain some details of our model. The fully compressible equations in quasi-flux form used in this study are here. This form was developed by Satomura and Akiba. Note that flux form equations are well suited to finite-volume discretization in view of conservation characteristics.

Shaved cell method (Adcroft et al. 1999)

Topography is approximated by a piecewise linear function on Cartesian grids.

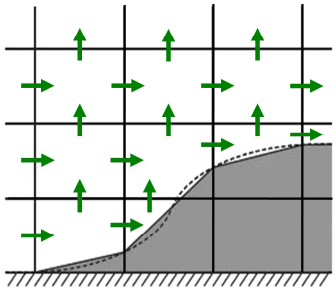

- Equations are discretized by the finite-volume method.
- Cartesian coordinate approaches do not suffer from truncation errors in terrain-following models.

Next, I will explain the shaved cell representation of topography which was originally proposed by Adcroft et al.. This method approximates topography by a piecewise linear function, and spatial discretization is carried out using the finite volume method. In the finite volume method, equations are descretized by flux exchanges among adjacent cells as indicated by these arrows. Because the shaved cell method uses Cartesian coordinates, it does not suffer from truncation errors in terrain-following models.

Key points in shaved cell modeling

(1) How to avoid severe restrictions on time steps due to small cut cells ?

- Small cut cells require small time steps to satisfy the CFL condition.
- We should avoid this severe restriction on time steps to keep the computational time reasonable.

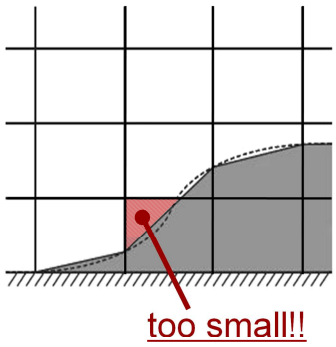

Now, there are two key points in shaved cell modeling. The first point is how to avoid severe restrictions on time steps due to small cut cells. Small cells cut by topography, such as this cell, require small time steps to satisfy the CFL condition. To keep the computational time reasonable, we should avoid this severe restriction on time steps in some way.

Key points in shaved cell modeling

(2) How to accurately evaluate the pressure gradient near the ground?

- In shaved cell model, some pressure points are underground.
- It happens that a cell may not have pressure points necessary to calculate the pressure gradient.
- Some models use a way to prognose underground pressure. (Tseng & Ferziger 2003, Walko & Avissar 2008)

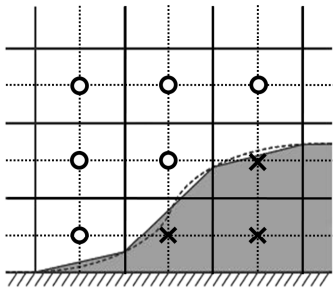

The second point is how to accurately evaluate the pressure gradient near the ground. In a shaved cell model, some pressure points are under the terrain surface. For example, if pressure points are arranged on cell centers, then the arrangement of pressure points looks like this. In this case, the circled points are in the fluid, but the crossed points are under the ground. We cannot obtain the pressure on underground points in a usual way, so it is possible that a cell near the boundary may not have all the pressure points necessary to calculate the pressure gradient. Though some models use a way to prognose the pressure values under the ground, we think that the use of the underground pressure values adversely impacts the flow dynamics near the ground.

Cell-combining approach
(e.g., Udaykumar et al. 1997; Ye et al. 1999)

Small cut cells are combined with neighboring cells either vertically or horizontally.

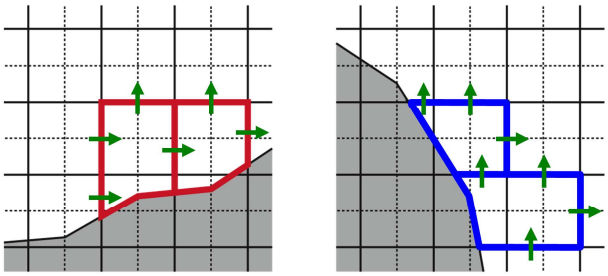

- Avoiding severe restriction by CFL criteria maintaining the rigid evaluation of cell volumes.
- It also keeps the model's conservation characteristics.

To solve the difficulties that I have explained, our method uses a cell combining approach used in Computational Fluid Dynamics. Here, small cells whose volume is smaller than half of a regular cell are combined with a neighboring cell. We use both vertical and horizontal combinations depending on slope angles. Small cells on gentle slopes are combined with upper cells like this, and small cells on steep slopes are combined with either each right or left cell in the fluid like this. Combined cells exchange flux with the adjacent cells in this way, and this combination process does not alter the model's conservation characteristics. Therefore, this approach can avoid severe restriction by CFL criteria maintaining the rigid evaluation of cell volumes, and also keeps the conservation characteristics.

A unique arrangement of variables
(Yamazaki and Satomura, submitted to MWR)

This arrangement enables simple computations of the pressure gradient without using underground values.

- Velocity components on the topographic boundary are diagnostically evaluated.
- The pressure gradient is only computed on the velocity cells with centers in the fluid, and all of them retain rectangular shapes.
- There is no need to combine velocity cells.

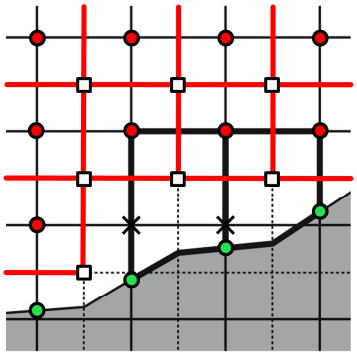

□ scalar variables
○ velocity components

In addition, we introduced a unique arrangement of variables to enable simple computations of the pressure gradient near the boundary without using underground values. In our method, scalar variables are arranged on the cell centers. On the other hand, velocity components are arranged on the corners of the cells. Note that velocity components are not arranged on the intermediate points of the combined faces, such as these crosses. Then, velocity components on the boundary, indicated by green circles, are diagnostically evaluated. For example, when the non-slip boundary condition is imposed, all these velocity values are set to zero. When the free-slip boundary condition is imposed, a boundary velocity is extrapolated from the velocities surrounding the boundary point. Then, the pressure gradient is only computed on the velocity cells with centers in the fluid, indicated by red circles, and all cells corresponding to these centers retain rectangular shapes. So, the evaluation of the pressure gradient is straightforward. For example, the pressure gradient on this velocity cell is simply computed from these four pressure points. The calculation of the pressure gradient on the other velocity cells is performed in the same way. Therefore, with this method, the pressure gradient can be calculated simply, accurately and without any difficulty. Further, there is no need to combine velocity cells, thus we can keep the computational costs of combining cells as low as non-staggered models.

Model descriptions of “Sayaca-2D”

■ **Dynamics**	
Dimension	2-D
Governing equations	Fully compressible non-hydrostatic system
Spatial discretization	Finite volume method
Time integration	Leap frog with Asselin filter
Temporal scheme	All explicit
Topography	Shaved cell method with a cell-combining approach
■ **Physics**	
Subgrid turbulence parametarization	1.5 order (Klemp and Wilhelmson,1974)

Other descriptions of our model are here. Green colored figures are characteristics of our model. The leap-flog scheme with the Asselin filter is used for the time integration. We integrate everything explicitly. For the subgrid turbulence parametarization, 1.5 order closure model is used.

Numerical examples of mountain waves

Two-dimensional numerical simulations of flow over a mountain are performed using the developed model.

(1) Flow over a bell-shaped mountain

U_o = 10 ms^{-1} N = 0.01 s^{-1}

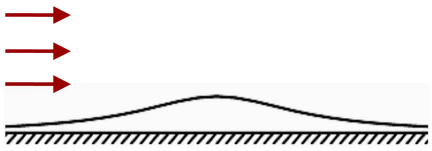

a = 5 km, h = 100 m

(2) Flow over a semicircular mountain

U_o = 10 ms^{-1} N = 0.01 s^{-1}

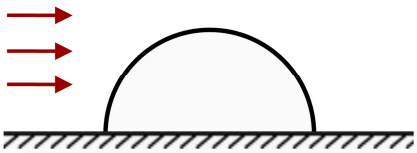

r = 1 km

Now, let me talk about results. We performed two-dimensional numerical simulations of flow over a mountain using the developed model. Here, two mountains are used. One is a low bell-shaped mountain with gentle slopes. The other is a semicircular mountain which has very steep slopes at the foot. The constant horizontal velocity and Brunt-Vaisala frequency are specified for both cases.

(1) Flow over the bell-shaped mountain

(a = 5 km, h = 100 m, Δx = 1 km, Δz = 50 m)

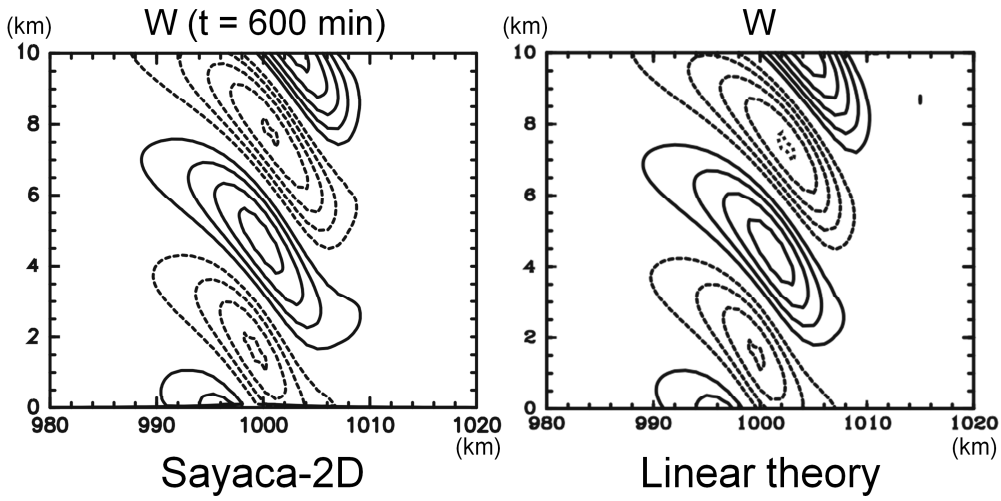

(contour interval : 0.05 ms^{-1})

This is the result in the case of the bell-shaped mountain after attainment of quasi-steady state. The horizontal and vertical grid intervals that we used are 1 km and 50 m, respectively. This shows the vertical velocity field calculated by our model, and this shows that by the linear theory. The vertical velocity calculated by the model agrees well with that in the analytical solution.

(1) Flow over the bell-shaped mountain

(a = 5 km, h = 100 m, Δx = 1 km, Δz = 50 m)

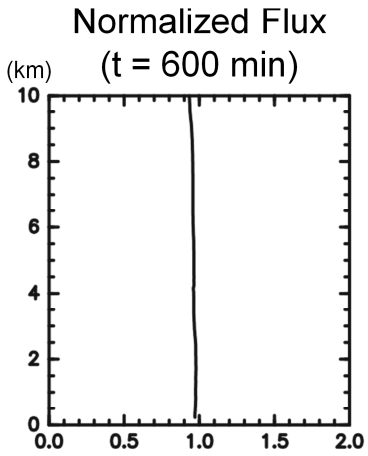

Sayaca-2D reproduces a sufficiently accurate flow over gentle slopes.

This is the momentum flux in our model normalized by that in the linear theory. It is nearly uniform from near the surface to 10 km, thus the momentum flux in model agrees well with that in the linear theory. Thus we conclude that our model reproduces a sufficiently accurate flow over gentle slopes.

(2) Flow over the semicircular mountain

(r = 1 km, $\Delta x = \Delta z$ = 500 m)

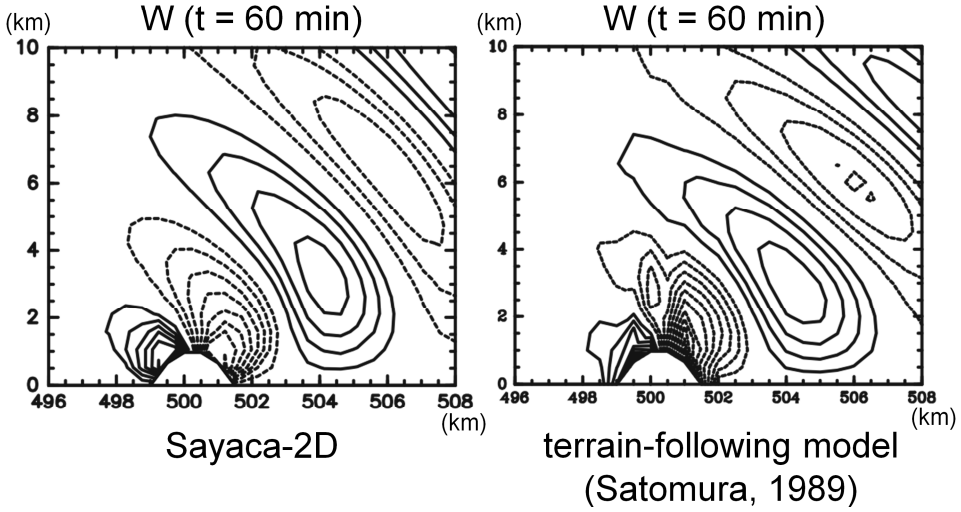

(contour interval : 1 ms^{-1})

Next, this is the result in the case of the semicircular mountain after attainment of quasi-steady state. Here, both the horizontal and vertical grid intervals are 500 m.

This shows the vertical velocity field calculated by Sayaca-2D, and this shows that by the terrain-following model developed by Satomura. The vertical velocity field in the shaved cell model is clearly less noisy than that in the terrain-following model.

(2) Flow over the semicircular mountain

(r = 1 km, $\Delta x = \Delta z$ = 500 m)

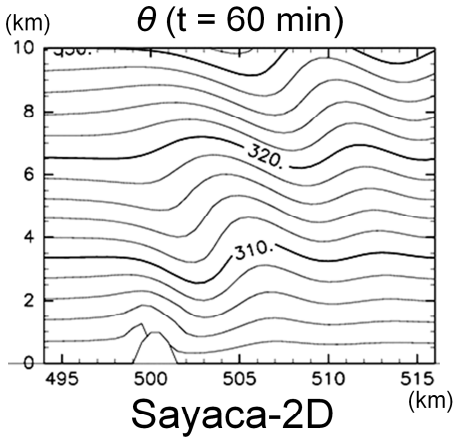

Sayaca-2D

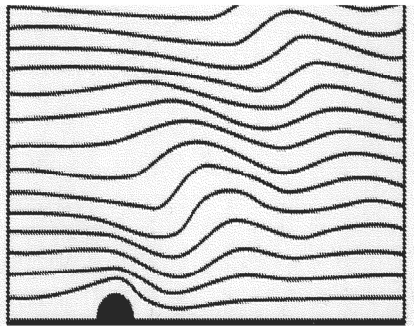

analytical solution
(Miles & Huppert, 1986)

Sayaca-2D can reproduce smooth and accurate flows over gentle as well as steep slopes.

Finally, this shows the potential temperature field in our model, and this shows the stream lines of the analytical solution given by Miles & Huppert. They are similar to each other and it shows that our model reproduces an accurate flow over the semi-circular mountain. Therefore, we conclude that our model can reproduce smooth and accurate flows over gentle as well as steep slopes, thus it is appropriate and sufficiently accurate for simulations of flow over complex terrain.

Summary

A new 2-D nonhydrostatic atmospheric model code-named “Sayaca-2D” was developed.

- The shaved cell method is used along with a cell-combining approach.
- A unique staggered arrangement of variables enables quite simple computations of the pressure gradient near the boundary.
- Sayaca-2D reproduced smooth and accurate flows over gentle as well as steep slopes, where significant errors are observed in a terrain-following model.

Now, let me summarize my talk. In the present study, we developed a new non-hydrostatic atmospheric model code-named “Sayaca-2D”. We use the shaved cell method as a representation method of topography on Cartesian grids, and use a cell combining approach to avoid severe restrictions on time steps. We devised our own unique arrangement of variables that greatly simplifies computations of the pressure gradient near the boundary. Two-dimensional numerical simulations of mountain waves were performed showing that our model reproduced smooth and accurate mountain waves over gentle as well as steep slopes, thereby demonstrating the advantage of the current method for flows over complex terrain. As for the future, we hope to upgrade this model into a three dimensional model as soon as possible. Thank you very much for your attention.

Acknowledgement

This study was supported in part by a Grant-in-Aid for JSPS fellows. Part of this study was also supported by the MEXT Special Coordination Funds for Promoting Science and Technology “International Research for Prevention and Mitigation of Meteorological Disasters in Southeast Asia.”

Direct evaluation of the velocity components on the boundary

With the non-slip boundary condition

- All velocity values on the boundary are set to zero.

With the free-slip boundary condition

- The component of the velocity that is tangential to the surface is preserved.
- For example, the velocity at the boundary point A is extrapolated as

$$\mathbf{v}_A = \mathbf{v}_P - (\mathbf{v}_P \cdot \mathbf{n}_A)\mathbf{n}_A$$

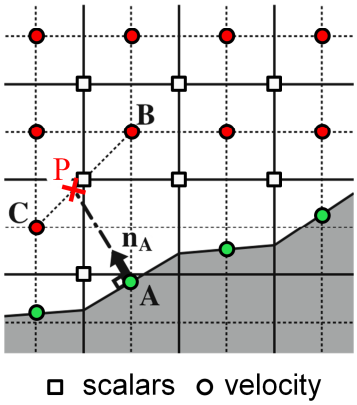

where $\mathbf{n}_A$ indicates the unit normal direction to the surface, and $\mathbf{v}_P$ is the mean velocity above the normal direction calculated as

$$\mathbf{v}_P = \frac{\mathbf{v}_B \cdot \overline{\mathrm{PC}} + \mathbf{v}_C \cdot \overline{\mathrm{PB}}}{\overline{\mathrm{BC}}}$$

In our method, the velocity components on the boundary, indicated by green circles, are diagnostically evaluated. When the non-slip boundary condition is imposed, all velocity values on the boundary are set to zero. With the free-slip boundary condition, boundary velocity values are extrapolated from velocities at red points. At this time, the component of the velocity that is tangential to the surface is preserved. For example, the velocity at the boundary point “A” is extrapolated from the velocities at points “B” and “C”. First, we calculate the velocity at point “P” above the normal direction to the surface at point “A” by linear interpolation between the velocities at points “B” and “C” as this, and calculate the boundary velocity at point “A” using this velocity like this. This part is the normal component of the velocity at point “P”, and subtract the normal component from the total velocity, then we can obtain the tangential component. We regard this tangential component as the boundary velocity. The other boundary velocities are calculated in the same way.

Flux calculations on combined cells

- The cell *O* enclosed by the area *ABCD* exchanges flux with the cells, *N*, *E*, *W*, and *SW*.
- Zero normal flow is assumed at the faces on the immersed boundary.
- The normal velocity of these fluxes is obtained by linear interpolation between the values on the ends of each face.

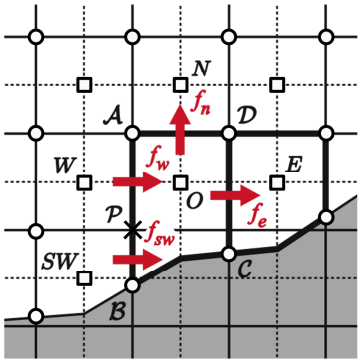

- The scalar quantity in these fluxes are approximated by the simple average of cell center values of the cells exchanging fluxes for computational simplification.

ex.) $$\int_{AB} f\,dz \approx f_w \cdot \overline{AP} + f_{sw} \cdot \overline{PB} = \frac{u_A + u_P}{2} \cdot \frac{\phi_O + \phi_W}{2} \cdot \overline{AP} + \frac{u_P + u_B}{2} \cdot \frac{\phi_O + \phi_{SW}}{2} \cdot \overline{PB}$$

where $$u_P = \frac{u_A \cdot \overline{PB} + u_B \cdot \overline{PA}}{\overline{AB}}.$$

Truncation errors in terrain-following models

- In terrain-following models, equations are discretized on a grid that conforms to the lower boundary.
- Horizontal gradient computation on a terrain-following grid essentially subject to truncation errors due to nonorthogonal coordinates.

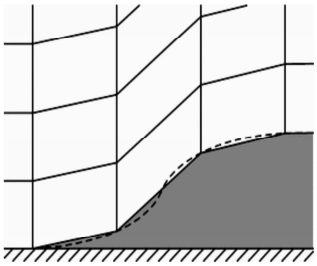

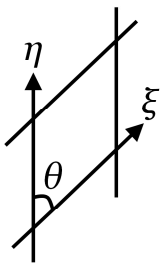

- The steeper the slope, the larger the errors T (Thompson et al. 1985).

$$T \approx \frac{1}{2}\left\{ -x_{\xi\xi} f_{xx} + \left(y_{\eta\eta} f_{yy} - x_{\xi\xi} f_{xy}\right) \underline{\cot\theta} \right\}$$

$T \propto \cot\theta$

- This errors will be serious in high-resolution simulations where steep slopes may appear.

Horizontal gradient computation on a terrain-following grid essentially subject to truncation errors, because the horizontal gradient at this cell, for example, is calculated from the values at these neighboring cells, and the deviation from the exact horizontal direction causes the errors described as this. The steeper the slope, the larger the deviation, and the larger the errors. You can get details from this book, Thompson et al..

Governing equations
(Satomura & Akiba, 2003)

$$\frac{\partial(\rho u)}{\partial t}+\frac{\partial(\rho uu)}{\partial x}+\frac{\partial(\rho uw)}{\partial z}=-\frac{\partial p'}{\partial x}+DIF(\rho u)$$
$$\frac{\partial(\rho w)}{\partial t}+\frac{\partial(\rho wu)}{\partial x}+\frac{\partial(\rho ww)}{\partial z}=-\frac{\partial p'}{\partial z}-\rho' g+DIF(\rho w)$$
$$\frac{\partial p'}{\partial t}=-\frac{R_d \pi}{1-R_d/C_p}\left\{\frac{\partial(\rho\theta u)}{\partial x}+\frac{\partial(\rho\theta w)}{\partial z}+DIF(\rho\theta)\right\}$$
$$\frac{\partial \rho'}{\partial t}+\frac{\partial(\rho u)}{\partial x}+\frac{\partial(\rho w)}{\partial z}=0$$

- Fully compressible quasi-flux form equations
- Flux form of the advection terms is superior to advective form in the view of conservation characteristics.
- This form does not suffer from the cancellation error because of subtracting the hydrostatic variable ($\overline{p}$ or $\overline{\rho}$) from the nearly hydrostatic total variable (p or ρ).

In these equations, the advection terms are written in flux form. Flux form is superior to advective form because of the conservation of advected quantity. The advection terms in the conservation equation for potential temperature are not completely in flux form, so this form is classified as a “quasi-flux” from. By directly prognosing deviations from the hydrostatic variable, the dashed variables, this form has the advantage that it does not suffer from the cancellation error because of subtracting the hydrostatic variable from the nearly hydrostatic total variable.

Limits on topographic complexity

- ✕ A sharp-pointed mountain
- ✕ A steep v-shaped valley

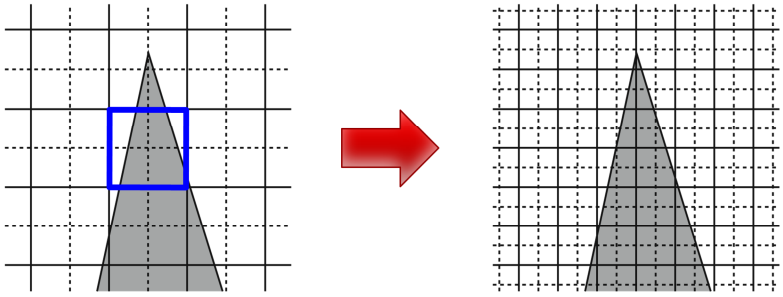

The fluid part of a cell is cut into two distinct pieces

Increase the resolution while keeping the shape of topography fixed

- In this study, we are not concerned with long thin topography such as a sharp-pointed mountain or a steep v-shaped valley where topography varies substantially on the grid scale.
- A way to handle long thin topography is to increase the resolution while keeping the shape of topography fixed.

In this study, we are not concerned with long thin topography such as a sharp-pointed mountain or a steep v-shaped valley. For example, this sharp-pointed mountain cuts a cell into two distinct pieces, and our method is not applicable to this situation. A way to handle long thin topography is to increase the resolution while keeping the shape of topography fixed like this to avoid topographic changes on the grid scale.

However, this approach has not yet been implemented or tested in our model. We are still thinking about this problem.

Combining rules

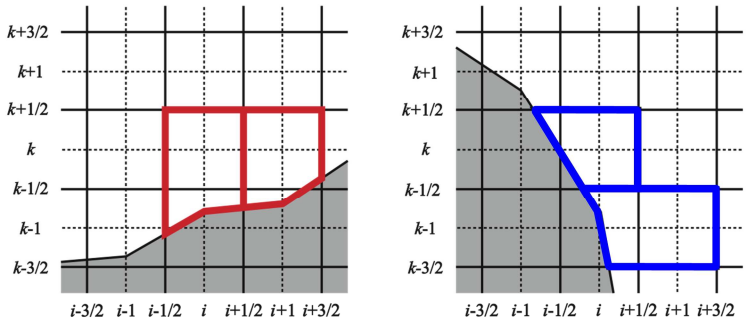

- The following cells are combined with a neighboring cell.
  - Cut cells whose volume is smaller than $\Delta x \Delta z / 2$.
  - Cut cells whose center is underground.
- The direction of cell combination is determined by mean slope angle:

$$\alpha_{i,k} = \tan^{-1}\left(\frac{h_{i+1/2} - h_{i-1/2}}{\Delta x}\right) .$$

- If $|\alpha| \le \tan^{-1}(\Delta z / \Delta x)$, small cut cells are combined with each upper cell; else, they are combined with either each right or left cell in the fluid.

Comparative simulations over a pyramidal mountain

(Δx = 500 m, Δz = 200 m)

W (t = 120 min)

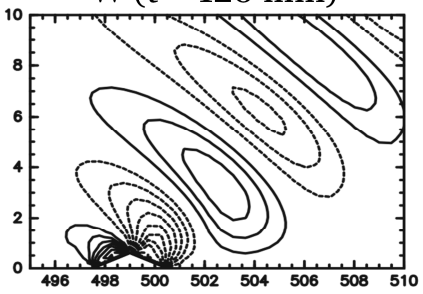

vertical combinations only

W (t = 120 min)

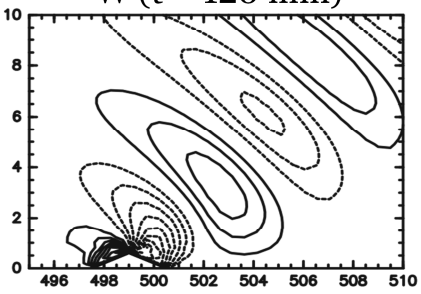

horizontal combinations only

- To confirm that the two combinations produce consistent results, two physically identical simulations are performed.
- A pyramidal mountain with a slope angle $|\alpha| = \tan^{-1}(\Delta z / \Delta x)$ is used.
- The results of the two simulations are practically the same, and vertical as well as horizontal combinations work properly.

Three-dimensional modeling

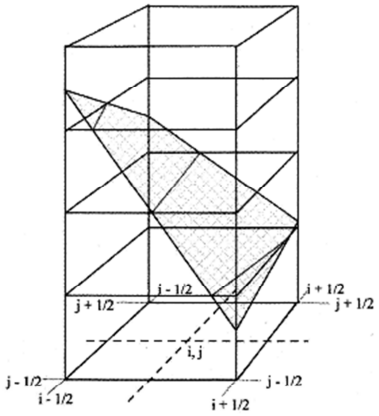

- The extension of our method to three dimensions should be straightforward.
- For establishing of a three-dimensional orographic surface, we will use a series of two-dimensional bilinear surface (Steppeler et al. 2006; Lock 2008).

How to obtain high near-ground vertical resolution ?

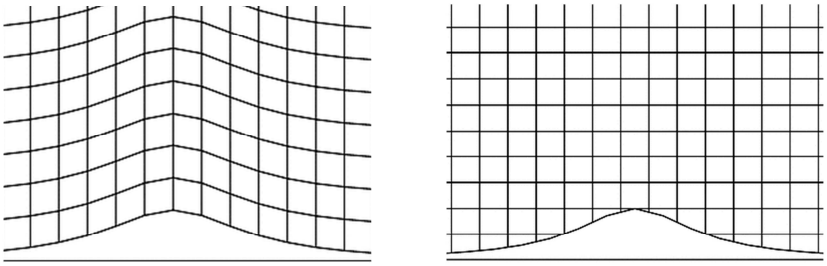

- With terrain-following coordinates, high vertical resolution near the ground is obtained over all topography heights with only a few additional levels.
- However, with Cartesian coordinates, a number of model levels are required to obtain high near-ground vertical resolution over a wide range of topographic heights.
- Further work is intended to solve this issue.

Himarayan terrain map (50m/mesh)